angles regarding those atoms appear within regularly accepted limits.

Acknowledgment. We thank the National Science Foundation (CHE 86-03055 and 89-09060) for support of this work, the Johnson Matthey Co., Inc. for a generous loan of rhodium salts, and Prof. T. Don Tilley of UCSD for communicating results to us prior to publication.

Supplementary Material Available: Tables of refined positional parameters, anisotropic thermal parameters, calculated hydrogen positional parameters, and complete bond distances and angles for non-hydrogen atoms for **3b** and **10b** (18 pages); listing of observed and calculated structure factors for **3b** and **10b** (31 pages). Ordering information is given on any current masthead page.

Structure and Reactivity of Organochromium Macrocycles with Iodine by Chain and Electrophilic Mechanisms

Shu Shi, James H. Espenson,* and Andreja Bakac*

Contribution from Ames Laboratory and the Department of Chemistry, Iowa State University, Ames, Iowa 50011. *Received July 19, 1989*

Abstract: The kinetic studies on the reaction of $[RCr([15]aneN_4)(H_2O)]^{2+}$, hereafter $RCrL(H_2O)^{2+}$ (R = CH_3, C_2H_5, 1-C_3H_7, 1-C_4H_9, 4-$BrC_6H_4CH_2$), macrocycles with iodine show that the reactivity changes as a function of the nature of the organic group bound to chromium(III). In the case of primary alkylchromium(III) macrocycles, the reaction proceeds strictly by bimolecular electrophilic substitution. The specific rates are 4.7×10^3 M^{-1} s^{-1} (R = CH_3), 81 (C_2H_5), 12 (1-C_3H_7), 8.9 (1-C_4H_9), and 9.5 (4-$BrC_6H_4CH_2$). In the case of aralkylchromium(III) and secondary alkylchromium(III) macrocycles, however, both the normal electrophilic substitution and an oxidatively induced chain reaction mechanism are operative. Details of the chain reaction for R = $BrC_6H_4CH_2$ are reported. The rate constant for the formation of 4-$BrC_6H_4CH_2CrL(H_2O)^{2+}$ from $CrL(H_2O)^{2+}$ and 4-$BrC_6H_4CH_2Br$ was also determined, $k = 3.7 \times 10^4$ M^{-1} s^{-1}. The crystal and molecular structure of [4-$BrC_6H_4CH_2CrL(H_2O)]^{2+}(ClO_4)_2$·THF was determined. The molecule crystallizes in the space group $P2_1/c$. Cell parameters are $a = 11.683$ (3) Å, $b = 8.816$ (3) Å, $c = 29.959$ (8) Å, and $\beta = 96.29$ (11)°. The chromium is octahedrally coordinated by four N atoms of the macrocyclic ligand at the equatorial positions and by the 4-$BrC_6H_4CH_2$ and a water molecule at the axial positions.

The cleavage of metal–carbon bonds by halogens has been fairly widely studied.[1] Generally, two mechanisms are operative. One is electrophilic substitution, often an S_E2 process, that cleanly converts reactants to products. This is usually accompanied by inversion of stereochemistry at the α-carbon atom if the substrate is a transition-metal complex with a high coordination number. The S_E2 mechanism is a two-electron process that occurs without the intervention of reaction intermediates. The second mechanism is a one-electron-transfer process, in which the initial step is the formation of a caged radical pair (RM^+, $X_2^{\bullet-}$). The electron-transfer step may initiate a chain sequence for halogenolysis.

The literature in the field includes extensive studies on a series of organochromium complexes, $(H_2O)_5CrR^{2+}$,[2] and macrocyclic complexes of cobalt, including the cobaloximes, $RCo(dmgH)_2B$ (B = H_2O, pyridine, etc.).[3-6] The former complexes adopt an S_E2 mechanism for halogenolysis, whereas the mechanism for the cobaloximes includes an electron-transfer step. The participation of inorganic transition-metal complexes in photoinduced chain reactions was also noticed before.[7]

We have turned our attention to iodinolysis reactions of a different group of organometallic complexes. This is a series of alkyl and aralkyl derivatives of a chromium macrocycle, $RCr([15]aneN_4)H_2O^{2+}$.[8] Cleavage of the carbon–chromium bond in such complexes by electrophilic mercury(II) ions occurs strictly by an S_E2 mechanism.[9] Halogenolysis reactions have not been previously investigated for these complexes. Rather to our surprise, we find that the mechanism for the reaction of $RCr([15]aneN_4)H_2O^{2+}$ with I_2 changes along the series of R groups and both electrophilic and oxidative mechanisms have to be considered. We present the results of kinetic investigations in this paper.

No crystal structure data were available for the complexes $RCr([15]aneN_4)H_2O^{2+}$ until now. In this work we have determined by X-ray diffraction the structure of the perchlorate salt of the complex with R = 4-bromobenzyl. Among other factors, we were interested in establishing the identity of the compound on more secure grounds, in the extent of steric hindrance at the chromium–carbon bond, and in the ground-state steric influence, as measured by the extent of the elongation of the bond to the trans water molecule.

Experimental Section

Materials. The chromium(II) complex, CrL^{2+} (L = [15]aneN$_4$), was prepared by mixing stoichiometric amounts of $CrCl_2 \cdot 4H_2O$[10] and ligand L (Strem Chemical Co.) in aqueous solution.[8] The organochromium

(1) Kochi, J. K. *Organometallic Mechanisms and Catalysis*; Academic Press: New York, 1978; Chapter 18.
(2) (a) Espenson, J. H.; Williams, D. A. *J. Am. Chem. Soc.* **1974**, *96*, 1008. (b) Chang, J. C.; Espenson, J. H. *J. Chem. Soc., Chem. Commun.* **1974**, 233. (c) Espenson, J. H.; Samuels, G. J. *J. Organomet. Chem.* **1976**, *113*, 143.
(3) (a) Halpern, J.; Topich, J.; Zamaraev, K. I. *Inorg. Chim. Acta* **1976**, *20*, L21. (b) Topich, J.; Halpern, J. *Inorg. Chem.* **1979**, *18*, 1339.
(4) (a) Dreos, R.; Tauzher, G.; Marslch, N.; Costa, G. *J. Organomet. Chem.* **1975**, *92*, 227. (b) Dreos-Garlatti, R.; Tauzher, G.; Costa, G. *J. Organomet. Chem.* **1977**, *139*, 179. (c) Dreos-Garlattl, R.; Tauzher, G.; Costa, G. *J. Organomet. Chem.* **1979**, *182*, 409.
(5) (a) Okamoto, T.; Goto, M.; Oka, S. *Inorg. Chem.* **1981**, *20*, 899. (b) Fukuzumi, S.; Ishikawa, K.; Tanaka, T. *Chem. Lett.* **1986**, 1801. (c) Fan-chiang, Y.-T. *Organometallics* **1985**, *4*, 1515. (d) Fukuzumi, S.; Goto, T.; Ishikawa, K.; Tanaka, T. *J. Chem. Soc., Chem. Commun.* **1989**, 260.
(6) Toscano, P. J.; Barren, E.; Seligson, A. L. *Organometallics* **1989**, in press.
(7) Fukuzumi, S.; Nishizawa, N.; Tanaka, T. *Bull. Chem. Soc. Jpn.* **1983**, *56*, 709.
(8) Samuels, G. J.; Espenson, J. H. *Inorg. Chem.* **1979**, *18*, 2587. [15]-aneN$_4$ = 1,4,8,12-tetraazacyclopentadecane.
(9) Samuels, G. J.; Espenson, J. H. *Inorg. Chem.* **1980**, *19*, 233.
(10) Holah, D. G.; Fackler, J. P., Jr. *Inorg. Synth.* **1969**, *10*, 26.

0002-7863/90/1512-1841$02.50/0

Table I. Crystallographic Data for $[4\text{-}BrC_6H_4CH_2CrL(H_2O)](ClO_4)_2\cdot THF$

formula	$CrBrCl_2O_{10}N_4C_{22}H_{42}$
fw	725.41
space group	$P2_1/c$ (No. 14)
a, Å	11.683 (3)
b, Å	8.816 (3)
c, Å	29.959 (8)
β, deg	96.29 (1)
V, Å^3	3067 (3)
Z	4
d_{calc}, g/cm^3	1.571
crystal size, mm	0.30 × 0.14 × 0.13
μ(Mo Kα), cm^{-1}	18.84
data collcn instrument	Enraf-Nonius CAD4
radiation (monochromated in incident beam)	Mo Kα (λ = 0.71073 Å)
orientation reflcns: no., range (2θ)	25. $14° < 2\theta < 32°$
temp, °C	22 ± 1
scan method	θ–2θ
data collcn range (2θ), deg	0–45
no. unique data total	4018
no. data with $F_o^2 > 2.5\sigma(F_o^2)$	1293
no. of param refined	163
transmissn factors: max, min (ψ-scans)	1.00, 0.93
R^a	0.0806
$R_w{}^b$	0.0943
quality-of-fit indicator^c	1.66
largest shift/esd, final cycle	0.15
largest peak, e/Å^3	0.69

$^a R = \sum||F_o| - |F_c||/\sum|F_o|$. $^b R_w = [\sum w(|F_o| - |F_c|)^2/\sum w|F_o|^2]^{11.1}$; $w = 1/[\sigma^2(|F_o|) + 0.001|F_o|^2]$. ^{c}Quality-of-fit = $[\sum w(|F_o| - |F_c|)^2/(N_{observns} - N_{param})]^{11.2}$.

complexes, $RCrL(H_2O)^{2+}$ (R = CH_3, C_2H_5, 1-C_3H_7, 1-C_4H_9), were prepared from CrL^{2+} and the corresponding organic bromide following the published procedure.[8] Similarly, *sec*-alkyl and aralkyl complexes were prepared from the organic halides. All organochromium macrocycles were separated and purified by ion exchange on Sephadex C-25. Iodine solutions were prepared by dissolving the AR-grade reagent in 0.01 M perchloric acid.

Iodine and triodide ion concentrations were determined spectrophotometrically at 467 nm (ϵ 733 M^{-1} cm^{-1} for I_2) and 352 nm (2.46 × 10^4 M^{-1} cm^{-1} for I_3^-).[11] The extinction coefficients for $RCrL(H_2O)^{2+}$ were taken from the literature.[8] UV data [λ, nm (ϵ, M^{-1} cm^{-1})]: R = CH_3, 258 (3.30 × 10^3), 375 (2.27 × 10^2); R = C_2H_5, 264 (3.10 × 10^3), 383 (3.87 × 10^2); R = 1-C_3H_7, 265 (3.44 × 10^3), 383 (4.65 × 10^2); R = 1-C_4H_9, 268 (3.30 × 10^3), 383 (4.59 × 10^2). The molar absorptivities listed were used to determine the concentrations of the organochromium ions. The new complex prepared in this work, $4\text{-}BrC_6H_4CH_2CrL(H_2O)^{2+}$, has maxima at 245 nm ($\epsilon$ 1.07 × 10^4 M^{-1} cm^{-1}), 281 (9.82 × 10^3), 303 (8.83 × 10^3), and 361 (2.40 × 10^3).

Kinetics. The kinetics of the reaction of $CrL(H_2O)^{2+}$ with $4\text{-}BrC_6H_4CH_2Br$ were followed at room temperature at 305 nm with a Durrum-Dionex stopped-flow spectrophotometer. Anaerobic conditions were required by the extreme sensitivity of the chromium(II) complex toward oxygen.

The kinetic study of the chain reaction between I_2 and $4\text{-}BrC_6H_4CH_2CrL(H_2O)^{2+}$ was conducted with the chromium complex in excess over iodine in solutions containing free iodide. The progress of the reaction was monitored by following the disappearance of I_3^- at λ 352 nm. The kinetics of the electrophilic reactions of the primary alkyl complexes were studied under pseudo-first-order conditions with $RCrL^{2+}$ in excess (R = CH_3, C_2H_5, 1-C_3H_7, 1-C_4H_9). For the case of R = 1-C_3H_7 the results were also checked with I_2 in excess. All reactions with I_2 were conducted at 25.0 ± 0.1 °C at a constant ionic strength of 0.20 M controlled by $NaClO_4$ and a constant pH of 2.00 controlled by perchloric acid.

Crystal Growth. Orange crystals of $[4\text{-}BrC_6H_4CH_2CrL(H_2O)](ClO_4)_2\cdot THF$ were grown from a sample of the purified organochromium cation in a mixture of THF and water in an ESR tube encapsulated within a sealed test tube. This system was employed to slow the temperature change as the solution was being cooled. This procedure afforded crystals suitable for X-ray diffraction.

X-ray Data and Structure. A crystal of approximate dimensions 0.30 × 0.14 × 0.13 mm was used to collect X-ray diffraction data with an Enraf-Nonius CAD-4 diffractometer. The cell constants were determined from reflections found by an automated search routine. An empirical absorption correction was based on a series of ψ-scans. Pertinent results are given in Table I.

The positions of Cr, Br, and Cl atoms were taken from an E-map produced by direct methods. Trial positions of other atoms were determined by a difference Fourier map and subsequent least-squares refinement. Because of the disorder in perchlorate anions and THF molecules, as well as a relatively low observation to parameter ratio, the phenyl group was subsequently refined as a rigid hexagon with C–C bond lengths of 1.395 Å and the perchlorate ions as rigid tetrahedra with Cl–O bond lengths of 1.50 Å. On the basis of the difference map, two orientations were assigned to each of the two independent perchlorate groups, with occupancy factors of 0.46:0.54 and 0.81:0.19. Hydrogen atoms were not included in the refinement but were used for the determination of F_{calc}. Final R and R_w values are shown in Table I. All calculations were performed on a Digital Equipment Corp. Micro Vax II computer. The refinement was carried out with the SHELX-76 package.

Spectrum and Product Analysis. The UV/visible spectra were taken with a Perkin-Elmer Lambda Array 3840 UV/vis spectrophotometer. The I_3^- ion was identified spectrophotometrically. The organic products were identified with a Hewlett-Packard Model 5790 gas chromatograph with a 6-ft column packed with OV-101 stationary phase. The instrument was calibrated by use of standard organic halides.

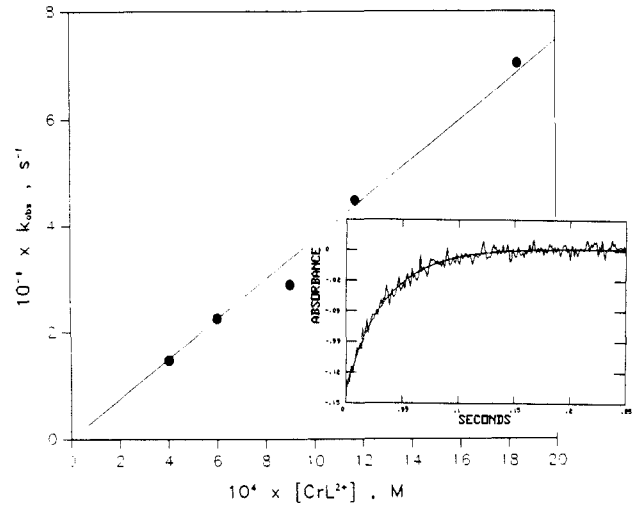

Figure 1. Plot for the reaction of $CrL(H_2O)^{2+}$ with $4\text{-}BrC_6H_4CH_2Br$ showing the variation of the pseudo-first-order rate constant k_{obsd} with the concentration of the chromium(II) macrocycle. The inset shows a stopped-flow kinetic trace for a run with $[CrL^{2+}]_0 = 9.0 \times 10^{-4}$ M and [RBr] = 8.8 × 10^{-6} M.

Results and Discussion

Formation of $4\text{-}BrC_6H_4CH_2CrL(H_2O)^{2+}$. The reaction between the $4\text{-}BrC_6H_4CH_2Br$ (RBr) and CrL^{2+} was studied in 10% ethanol–water, since the bromide is insoluble in strictly aqueous solution. CrL^{2+} was used in at least 10-fold excess over RBr. The reaction followed pseudo-first-order kinetics in each run, and the plot of k_{obsd} vs $[CrL^{2+}]$ was linear, as depicted in Figure 1. The second-order rate constant obtained is 3.73 × 10^4 M^{-1} s^{-1}.

The reaction produces the indicated organochromium(III) cation, as shown by its UV/visible spectrum (after separation by ion-exchange chromatography) and by X-ray crystallography. The rate constant of 3.7 × 10^4 M^{-1} cm^{-1} is slightly higher than the value for $PhCH_2Br$, k = 1.9 × 10^4 M^{-1} s^{-1}.[8] This small difference is consistent with the proposed free-radical mechanism for such reactions:

$$CrL(H_2O)_2^{2+} + RBr \rightarrow BrCrL(H_2O)^{2+} + R^\cdot + H_2O \qquad k_1 \quad (1)$$

$$CrL(H_2O)_2^{2+} + R^\cdot \rightarrow RCrL(H_2O)^{2+} + H_2O \qquad k_2 \text{ (fast)} \quad (2)$$

According to this scheme, $-d[RBr]/dt = k_1[CrL^{2+}][RBr]$. Thus, the values of the rate constants cited above represent k_1. The 4-Br derivative is expected to react more rapidly than the unsubstituted benzyl complex owing to the electron-withdrawing

(11) Awtry, A. D.; Connick, R. E. *J. Am. Chem. Soc.* **1965**, *87*, 5026.

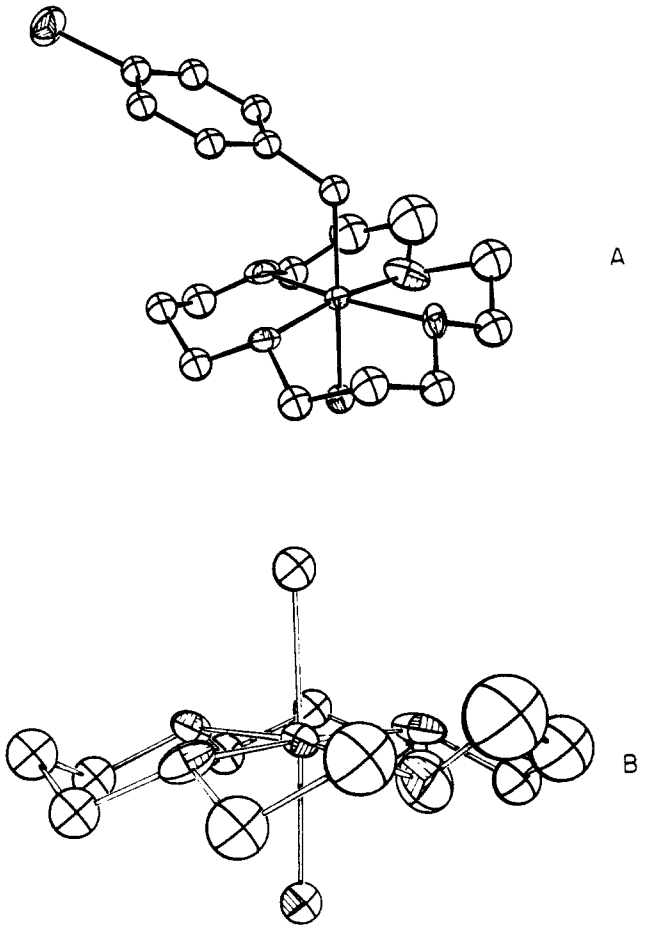

Figure 2. ORTEP diagram of the (bromobenzyl)chromium macrocycle showing (A) the molecular structure of the cation and (B) the primary coordination shell of the chromium, with emphasis of the distinction between sides A (above) and B (below).

properties of bromine and resonance stabilization of the alkyl radical by the *p*-bromine.

The complex 4-$BrC_6H_4CH_2CrL(H_2O)^{2+}$ is more stable toward air than $PhCH_2CrL(H_2O)^{2+}$. In both cases the reaction proceeds by unimolecular homolysis.[12] The electron-withdrawing effect of the *p*-bromine makes the Cr–C bond more polar, thereby retarding the homolysis. The complex 4-$BrC_6H_4CH_2CrL(H_2O)^{2+}$ is quite stable toward acid; it can be stored in solution at pH 2 and 0 °C for weeks.

The crystal structure of [*p*-$BrC_6H_4CH_2CrL(H_2O)$]$(ClO_4)_2$·THF is shown in Figure 2. The cation adopts a distorted octahedral structure with a molecule of water trans to the Cr–C bond. The relevant bond lengths and bond angles are summarized in Table II. The Cr–C bond length (2.14 Å) in this cation is slightly longer than the reported values of other stable organochromium complexes (2.06 Å in *trans*-[$(CH_2Cl)Cr(acac)_2·H_2O$] and 2.077–2.129 Å in *trans*-$RCr(acac)_2py$, for R = $CHCl_2$ and CH_2Cl, respectively).[13,14] The Cr–C(1)–C(2) angle of 123° is also larger than that for a typical sp^3 carbon. All of these deviations are due to the steric repulsion between the *p*-bromobenzyl group and the bulky macrocyclic ligand. Similar distortions have been observed before.[13,14] We also note the large Cr–C–Si bond angle (127.9–128.3°) in the compound *cis*-[$Me_3SiCH_2Cr(bipy)$]I.[15]

It is noted from Figure 2 that the coordinated nitrogens adopt a configuration with three of the four N–H bonds pointing upward and one downward. This asymmetric configuration makes the two sides of the CrN_4 plane different (designated as side A and side B, respectively, in Figure 2). A space-filling model shows that this asymmetric binding of [15]aneN_4 to chromium(III) results in the A side being less crowded than the B side. It is therefore not too surprising that the 4-bromobenzyl group binds preferentially to the A side even though the CrN_4 plane is quite flat.

A comparison between the Cr^{III}–OH_2 bond length in *trans*-4-$BrC_6H_4CH_2CrL(H_2O)^{2+}$ (2.13 Å) and that in *trans*-$ClCrL(H_2O)^{2+}$ (2.04 Å)[16] can also be made. The reported crystal structure of the chloro complex has the H_2O molecule bound to the more open A side, rather than the B side as in the case of the organometallic complex. Hence, both the trans influence of the Cr^{III}–C bond and the steric crowdedness of the B side might contribute to the elongation of the Cr^{III}–OH_2 bond in the 4-bromobenzyl complex.

Electrophilic Substitution Reactions with Iodine. All the primary alkylchromium complexes, $RCrL(H_2O)^{2+}$, are quite stable toward O_2. No reaction was observed in 60 min in oxygen-saturated solutions, $[RCrL(H_2O)^{2+}] \sim 3 \times 10^{-4}$ M. These solutions are also stable toward acidolysis. No significant reaction was observed in 60 min in solutions of $RCrL(H_2O)^{2+}$ containing 0.01–0.4 M $HClO_4$ at room temperature.

Table II. Bond Distances (Å) and Bond Angles (deg)

atom 1–atom 2	distance[a]	atom 1–atom 2	distance[a]
Cr–O(1)	2.13 (1)	C(3)–C(4)	1.48 (3)
Cr–N(1)	2.11 (2)	C(5)–C(6)	1.52 (3)
Cr–N(2)	2.08 (2)	C(6)–C(7)	1.56 (3)
Cr–N(3)	2.12 (2)	C(8)–C(9)	1.44 (4)
Cr–N(4)	2.08 (2)	C(9)–C(10)	1.60 (5)
Cr–C(1)	2.14 (2)	C(11)–C(12)	1.56 (4)
Br–C(24)	1.89 (1)	C(21)–C(22)	1.39 (2)
N(1)–C(2)	1.52 (3)	C(21)–C(26)	1.39 (2)
N(1)–C(12)	1.45 (3)	C(22)–C(23)	1.40 (1)
N(2)–C(4)	1.50 (3)	C(23)–C(24)	1.39 (2)
N(2)–C(5)	1.45 (3)	C(24)–C(25)	1.39 (2)
N(3)–C(7)	1.36 (3)	C(25)–C(26)	1.39 (1)
N(3)–C(8)	1.53 (3)	O(10)–C(31)	1.43 (3)
N(4)–C(10)	1.24 (5)	O(10)–C(34)	1.45 (3)
N(4)–C(11)	1.82 (4)	C(31)–C(32)	1.46 (4)
C(1)–C(21)	1.48 (2)	C(32)–C(33)	1.43 (5)
C(2)–C(3)	1.50 (3)	C(33)–C(34)	1.43 (5)
atom 1–atom 2–atom 3	angles	atom 1–atom 2–atom 3	angles
O(1)–Cr–N(1)	90.6 (6)	Cr–N(4)–C(10)	125 (2)
O(1)–Cr–N(2)	87.7 (5)	Cr–N(4)–C(11)	106 (1)
O(1)–Cr–N(3)	87.9 (6)	C(10)–N(4)–C(11)	87 (2)
O(1)–Cr–N(4)	83.1 (7)	Cr–C(1)–C(21)	123 (1)
O(1)–Cr–C(1)	178.0 (6)	N(1)–C(2)–C(3)	112 (2)
N(1)–Cr–N(2)	95.4 (7)	C(2)–C(3)–C(4)	113 (2)
N(1)–Cr–N(3)	168.9 (7)	N(2)–C(4)–C(3)	117 (2)
N(1)–Cr–N(4)	82.7 (7)	N(2)–C(5)–C(6)	114 (2)
N(1)–Cr–C(1)	88.7 (6)	C(5)–C(6)–C(7)	115 (2)
N(2)–Cr–N(3)	95.5 (8)	N(3)–C(7)–C(6)	111 (2)
N(2)–Cr–N(4)	170.6 (8)	N(3)–C(8)–C(9)	113 (2)
N(2)–Cr–C(1)	90.4 (8)	C(8)–C(9)–C(10)	133 (3)
N(3)–Cr–N(4)	86.2 (8)	N(4)–C(10)–C(9)	92 (3)
N(3)–Cr–C(1)	93.1 (7)	N(4)–C(11)–C(12)	96 (2)
N(4)–Cr–C(1)	98.7 (8)	N(1)–C(12)–C(11)	107 (2)
Cr–N(1)–C(2)	119 (1)	C(1)–C(21)–C(22)	122 (1)
Cr–N(1)–C(12)	112 (1)	C(1)–C(21)–C(26)	118 (1)
C(2)–N(1)–C(12)	110 (2)	Br–C(24)–C(23)	120 (1)
Cr–N(2)–C(4)	115 (1)	Br–C(24)–C(25)	120.0 (9)
Cr–N(2)–C(5)	115 (1)	C(31)–O(10)–C(34)	109 (2)
C(4)–N(2)–C(5)	109 (2)	O(10)–C(31)–C(32)	103 (2)
Cr–N(3)–C(7)	123 (2)	C(31)–C(32)–C(33)	106 (3)
Cr–N(3)–C(8)	112 (1)	C(32)–C(33)–C(34)	109 (3)
C(7)–N(3)–C(8)	109 (2)	O(10)–C(34)–C(33)	105 (3)

[a] Numbers in parentheses are estimated standard deviations in the least significant digits.

(12) Shi, S.; Bakac, A.; Espenson, J. H. To be published.
(13) Ogino, H.; Shoji, M.; Abe, Y.; Shimura, M.; Shimoi, M. *Inorg. Chem.* **1987**, *26*, 2592.
(14) Abe, Y.; Ogino, H. *Bull. Chem. Soc. Jpn.* **1989**, *62*, 56.
(15) Daly, J. J.; Sanz, F.; Sneeden, R. P. A.; Zeiss, H. H. *J. Chem. Soc., Dalton Trans.* **1973**, 1497. We appreciate a reviewer calling this paper to our attention.

(16) Samuels, G. J. Ph.D. Thesis, Iowa State University, 1979.

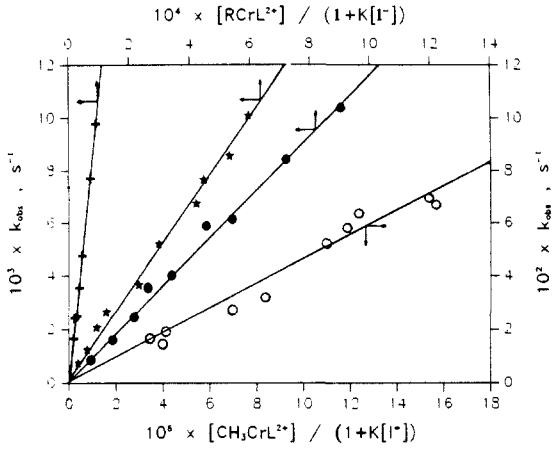

Figure 3. Plots of kinetic data for the reaction of alkylchromium macrocycles (R: Me, ○; C_2H_5, +; 1-C_3H_7, *; 1-C_4H_9, ●) with iodine in acidic solution showing the effects of the variation of the alkylchromium and iodide concentrations. $[RCrL_2(H_2O)^{2+}]_0 = (0.02\text{–}2.8) \times 10^{-3}$ M; $[I^-]_0 = (1.0\text{–}8.0) \times 10^{-3}$ M; $[I_2]_0 = (0.39\text{–}2.2) \times 10^{-5}$ M.

The Cr–C bond in $RCrL(H_2O)^{2+}$ can be easily cleaved heterolytically by I_2. Advantage was taken of the strong light absorption of I_3^- at 352 nm to monitor the reaction that proceeds according to the net equation (3). All the experiments were done

$$I_2 + RCrL(H_2O)^{2+} + H_2O \rightarrow I^- + RI + (H_2O)_2CrL^{3+} \quad (3)$$

in the presence of excess I^- to create the I_3^- chromophore. The reaction rate is first-order with respect to both iodine and alkylchromium concentrations, regardless of which one was used as the limiting reagent.

Since I_2 and I_3^- have almost identical reduction potentials, both should be considered as possible electrophiles. To distinguish between them, consider the rate laws in experiments with I_2/I_3^- as the limiting reagent. We consider three cases, in which K_f represents the formation constant of I_3^- and k_{obsd} the value of $-d \ln [I_2]/dt$. (1) I_3^- is the only active electrophile:

$$k_{obsd} = \frac{k_{I_3}K_f[I^-][RCrL(H_2O)^{2+}]}{1 + K_f[I^-]} \quad (4)$$

(2) I_2 is the only active electrophile:

$$k_{obsd} = \frac{k_{I_2}[RCrL(H_2O)^{2+}]}{1 + K_f[I^-]} \quad (5)$$

(3) Both I_3^- and I_2 are active electrophiles:

$$k_{obsd} = \frac{\{k_{I_3}K_f[I^-] + k_{I_2}\}[RCrL(H_2O)^{2+}]}{1 + K_f[I^-]} \quad (6)$$

The distinction between these cases clearly lies in the form of the dependence of k_{obsd} upon $[I^-]$. For all the primary alkylchromium complexes studied, the pseudo-first-order rate constant decreases as the free iodide concentration increases, as shown in Figure 3. The clear linearity in the plots of k_{obsd} versus $[RCrL(H_2O)^{2+}]/(1 + K_f[I^-])$ shows that only I_2 is the active electrophile and the rate law of eq 5 applies. Thus, I_3^- serves only as a chromophore useful in following the progress of the reaction and is in instantaneous equilibrium with I_2 ($I_3^- \rightleftharpoons I^- + I_2$). Consistent with that, the kinetics were unaffected by the variation of ionic strength in the range 5×10^{-3}–0.8 M.

The only organic product of the reaction was identified by gas chromatography as the alkyl iodide. As an independent test for the formation of RI, we conducted a two-stage reaction. In the first stage of this process, the reaction between I_2 and the organochromium macrocycle $RCrL(H_2O)^{2+}$ (here R = C_2H_5, 1-C_3H_7, and 4-$BrC_6H_4CH_2$) was carried out with a slight excess of the latter. Then a solution of $(H_2O)_2CrL^{2+}$ was added to react with any RI formed. Upon this addition the spectrum of $RCrL(H_2O)^{2+}$ quantitatively reappeared. This confirms the quantitative production of RI in the initial reaction with iodine as given in eq 3.

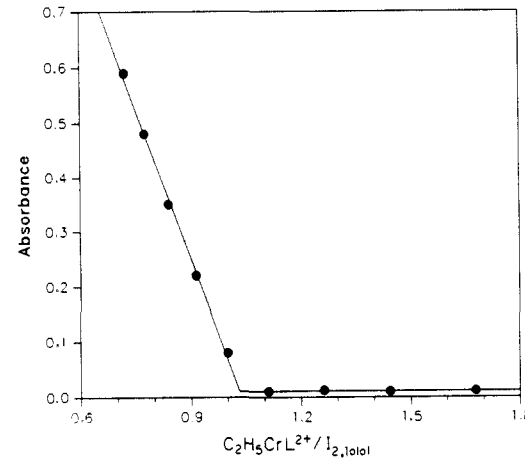

Figure 4. Titration of the ethylchromium macrocycle with iodine showing the end point at a 1:1 ratio. The absorbance was monitored at the 353-nm maximum of I_3^-.

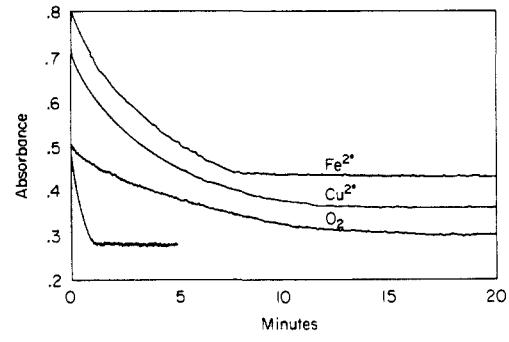

Figure 5. Kinetic traces for the reaction of I_2 (2.0×10^{-5} M) and 4-$BrC_6H_4CH_2CrL(H_2O)^{2+}$ (1.7×10^{-4} M). The unaffected chain reaction is shown along with reactions that are inhibited by O_2 (1.3×10^{-3} M), Cu^{2+} (4.0×10^{-3} M), and Fe^{2+} (3.7×10^{-4} M). Each run contained 4.0×10^{-3} M I^-.

Table III. Second-Order Rate Constants for the Electrophilic Cleavage of Chromium–Carbon Bonds of $RCr([15]aneN_4)H_2O^{2+}$ by Iodine[a]

R	k, M^{-1} s^{-1}
CH_3	4.7×10^3
C_2H_5	8.1×10^1
n-C_3H_7	1.2×10^1
n-C_4H_9	8.9×10^0
4-$BrC_6H_4CH_2$	$(9.5 \times 10^0)^b$

[a] In aqueous solution at 25.0 °C; ionic strength 0.2 M ($HClO_4$ + $NaClO_4$); $[H^+]$ = 0.010 M. [b] Electrophilic pathway only (see text).

Other lines of evidence supporting the mechanism were obtained from stoichiometric relationships. A spectrophotometric titration (Figure 4) shows the stoichiometric ratio of I_2 to $EtCrL(H_2O)^{2+}$ to be 1:1. The absorbance changes with either I_2 in excess (no free I^- added) or $RCrL(H_2O)^{2+}$ in excess (free I^- added) are consistent with the 1:1 stoichiometry. In the case of 1-$C_3H_7CrL(H_2O)^{2+}$, a kinetic study was also conducted with I_2 in excess (no free I^- added) affording the same second-order rate constant as shown in Table III.

The slopes in Figure 3 give the second-order rate constants for the bimolecular reaction between I_2 and $RCrL(H_2O)^{2+}$ (eq 3), as shown in the applicable rate law, eq 5. The second-order rate constants are summarized in Table III. The decrease in rate constant from R = Me ($k = 4.7 \times 10^3$ M^{-1} s^{-1}) to n-Bu (8.9 M^{-1} s^{-1}) is to be noted. In particular, this trend points to an S_E2 mechanism proceeding with inversion of configuration at carbon. The values reflect a trend in which the rate constant declines as the alkyl group gets bulkier because of increasing steric hindrance

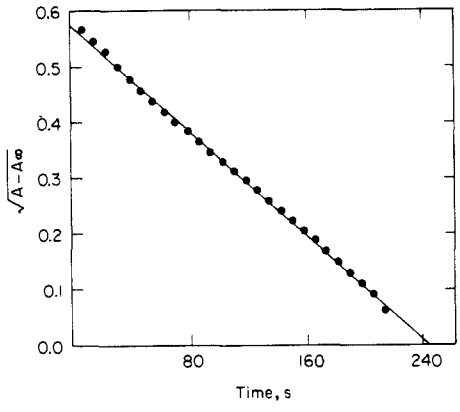

Figure 6. Plot showing the fit to pseudo-half-order kinetics in a reaction between I_2 (2.0×10^{-5} M) and 4-$BrC_6H_4CH_2CrL(H_2O)^{2+}$ (1.6×10^{-4} M) in the presence of I^- (4.0×10^{-3} M).

on the α-carbon from methyl to 1-butyl.[2]

Chain Reaction between 4-$BrC_6H_4CH_2CrL(H_2O)^{2+}$ and Iodine. When the chromium complex is present in excess ($\sim 10^{-4}$ M), the reaction is half-order with respect to the iodine concentration, as illustrated in Figures 5 and 6. Under those conditions, the presence of O_2 results in a much slower reaction and a pseudo-first-order kinetic profile. A decrease in the concentration of the chromium complex to $\sim 10^{-5}$ M, while the I_2 is kept in excess, also results in a pseudo-first-order trace even under strictly anaerobic conditions. The reaction proceeds much more rapidly when the chromium complex is used as excess reagent (at $\sim 10^{-4}$ M level) than it does when iodine is present in excess (at the same $\sim 10^{-4}$ M level). These observations suggest a free-radical chain pathway that requires a relatively high concentration of 4-$BrC_6H_4CH_2CrL(H_2O)^{2+}$ and anaerobic conditions to proceed.

Several extraneous reagents were used to diagnose the reaction mechanism. This entailed the addition of a substance (O_2, Cu^{2+}, Fe^{2+}) that might fulfill a chain-breaking role. Blank experiments confirmed the absence of a reaction between each of these reagents and the (bromobenzyl)chromium cation.

Addition of O_2 (<1 mM) or $CuCl_2$ (4 mM) significantly retarded the reaction and changed the appearance of the kinetic trace. Figure 5 illustrates the unaffected half-order absorbance–time profile along with ones with added O_2 and Cu^{2+}. Dioxygen is well-known to react rapidly with free radicals ($C_2H_5^\bullet + O_2 \rightarrow C_2H_5OO^\bullet$, for example, has $k = 4.7 \times 10^9$ M^{-1} s^{-1})[17] and presumably plays this chain-breaking role in the overall reaction scheme. The oxidation of benzyl radicals by Cu^{2+} has been established as well:[18]

$$PhCH_2^\bullet + Cu^{2+} + H_2O \rightarrow PhCH_2OH + Cu^+ + H^+ \quad (7)$$

The dramatic inhibitory effect of Cu^{2+} again points to the involvement of 4-$BrC_6H_4CH_2^\bullet$ radical in the chain reaction.

Addition of Fe^{2+} as $Fe(ClO_4)_2$(aq) (0.04–11 mM) effectively decreases the reaction rate as shown in Figure 5. The kinetic profile fits a fractional order between 0.5 and 1. The reaction

$$Fe^{2+} + I_2^- \rightarrow Fe^{3+} + 2I^- \quad (8)$$

with $k_8 = 6 \times 10^6$ M^{-1} s^{-1} [19] is believed to be the reason for the retardation by Fe^{2+}. Hence, $I_2^{\bullet-}$ is suggested as another chain-carrying radical intermediate.

A more detailed analysis of the kinetics of the chain reaction is now given. A plot of the instantaneous reaction rate versus the average concentration of I_2 in the interval as a double-logarithmic plot gave lines of slopes between 0.47 and 0.58. In other words, the order of the reaction with respect to $[I_2]$ appears to be $^1/_2$.

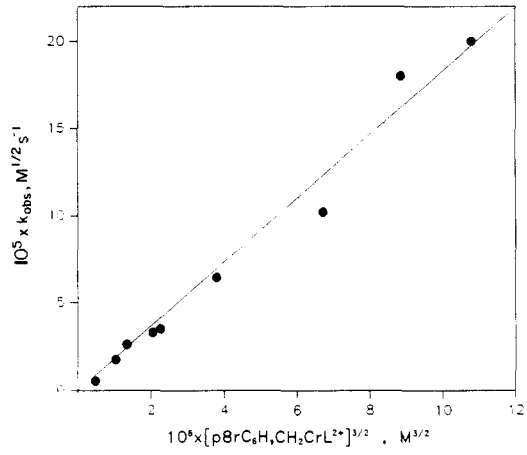

Figure 7. Plot illustrating the variation of the half-order rate constant with the $^3/_2$ power of the concentration of the bromobenzyl macrocycle. $[I_2] = 2 \times 10^{-5}$ M, $[I^-] = 2 \times 10^{-3}$ M.

The rate law at a constant concentration of the (bromobenzyl)-chromium complex is thus

$$-d[I_2]/dt = k_{obsd}[I_2]^{1/2} \quad (9)$$

This was tested by application of the integrated half-order equation; plots of the kinetic data as $(A_t - A_\infty)^{1/2}$ versus time give a straight line as depicted in Figure 6. The slope of the half-order plot is a function of the concentration of the excess (bromobenzyl)chromium reagent. A plot of ln k_{obsd} vs ln [4-$BrC_6H_4CH_2CrL(H_2O)^{2+}$] has a slope of 1.5, implying a kinetic order of the reaction with respect to organochromium complex concentration of $^3/_2$. The plot of k_{obsd} vs [4-$BrC_6H_4CH_2CrL(H_2O)^{2+}]^{3/2}$, shown in Figure 7, defines a straight line through the origin; its slope gives the rate constant $k_{10} = 18.3$ M^{-1} s^{-1}, as defined by eq 10.

$$\frac{-d[4\text{-}BrC_6H_4CH_2CrL(H_2O)^{2+}]}{dt} = k_{10}[I_2]^{1/2}[4\text{-}BrC_6H_4CH_2CrL(H_2O)^{2+}]^{3/2} \quad (10)$$

The chain mechanism proposed to account for the kinetic data is the following (with p-$BrC_6H_4CH_2CrL(H_2O)^{2+}$ = $RCrL^{2+}$):

$$RCrL^{2+} + I_2 \rightarrow RCrL^{3+} + I_2^{\bullet-} \quad (11)$$

$$RCrL^{3+} \rightarrow R^\bullet + CrL^{3+} \quad (12)$$

$$R^\bullet + I_2 + I^- \rightarrow RI + I_2^{\bullet-} \quad (13)$$

$$I_2^{\bullet-} + RCrL^{2+} \rightarrow RCrL^{3+} + 2\,I^- \quad (14)$$

$$2\,I_2^{\bullet-} \rightarrow I_3^- + I^- \quad (15)$$

The resulting net reaction, assuming that the kinetic chain is long, is

$$RCrL^{2+} + I_2 \rightarrow RI + CrL^{3+} + I^- \quad (16)$$

With the steady-state approximation for the concentrations of $I_2^{\bullet-}$ and the aralkyl radical, the rate expression associated with the mechanism given in eqs 11–15 is the following:

$$-d[RCrL^{2+}]/dt = k_{14}(k_{11}/k_{15})^{1/2}[RCrL^{2+}]^{3/2}[I_2]^{1/2} \quad (17)$$

The predominant organic product of the reaction was determined to be RI by the method herein previously described, in which the re-formation of $RCrL^{2+}$ was observed upon addition of the chromium(II) macrocycle. Further confirmation came from the observed absorbance change at 352 nm, which was consistent with the formation of RI in eq 13 and not (for example) ROH from a reaction such as $R^\bullet + I_2 + H_2O \rightarrow ROH + H^+ + I_2^{\bullet-}$.

The unique aspects of the mechanism are the oxidatively induced homolysis and the consequent participation of a chromium(IV) macrocycle in a kinetic chain. To our knowledge this is the first kinetically characterized reaction of RM in which the

(17) Rabani, J.; Pick, M.; Simic, M. *J. Phys. Chem.* **1974**, *78*, 1049.
(18) (a) Buxton, G. V.; Green, J. C. *J. Chem. Soc., Faraday Trans. 1* **1978**, *74*, 697. (b) Scaiano, J. C.; Leigh, W. J.; Ferraudi, G. *Can. J. Chem.* **1984**, *62*, 2355.
(19) Laurence, G. S.; Thornton, A. J. *J. Chem. Soc., Dalton Trans.* **1974**, 1142.

RM^+ species is a chain-carrying intermediate and homolysis of a transition-metal–carbon bond is involved in a chain-propagation process. Also, it should be noted that the mild oxidant I_2 reacts just sufficiently to initiate the kinetic chain (eq 11), and the much stronger oxidant $I_2^{\bullet}$ is required to cause chain propagation (eq 14).

Exploratory experiments were conducted on the reactions between iodine and other benzylchromium macrocycles and on two secondary alkyl complexes. Fractional-order kinetic behavior was also observed for R = $PhCH_2$, 4-$CH_3C_6H_4CH_2$, 2-C_3H_7, and 2-C_4H_9. We surmise that each of these reactions also proceeds by a chain mechanism, most likely as in eqs 11–15. Detailed measurements were not conducted in any of these cases, however.

One notes the facility of the oxidation of 4-$BrC_6H_4CH_2CrL(H_2O)^{2+}$ to the corresponding Cr(IV) complex, as shown in eq 11. Independent studies show that $RCrL(H_2O)^{2+}$ complexes, with R = aralkyl and secondary alkyl, are readily oxidized by various kinds of weak oxidants (e.g., Fe^{3+}, $ABTS^{\bullet-}$,[20] and Co^{III}(tetraeneN_4^+). These studies will be reported elsewhere.[12]

Bimolecular Electrophilic Substitution Reaction between 4-$BrC_6H_4CH_2CrL(H_2O)^{2+}$ and Iodine. All indications of a chain reaction disappear when the reaction is conducted under different concentration conditions. Evidently a new pathway becomes important. This occurs when the (bromobenzyl)chromium complex is used as the limiting reagent at sufficiently low concentrations ($\leq 10^{-5}$ M). Under these conditions the rate law appears to be first-order with respect to each reagent. The two pathways operate in parallel, and the complete rate law is

$$-d[RCrL^{2+}]/dt = k_{I_2}[I_2][RCrL^{2+}] + k_{10}[I_2]^{1/2}[RCrL^{2+}]^{3/2} \quad (18)$$

The relative importance of the two terms is governed mainly by the concentration of the organochromium complex. Experiments to evaluate the k_{I_2} term were conducted in the following concentration ranges: $[RCrL^{2+}]_0 = 1.9 \times 10^{-5}$ and $[I_2] = (0.33–1.1) \times 10^{-3}$ M. The kinetic data fit fairly well to pseudo-first-order kinetics, but not perfectly, since the fractional-order term is not entirely negligible. The value of k_{I_2} was estimated from the iodine variation and has the value of 9.5 M^{-1} s^{-1}. The product analysis shows that RI is the only organic product both in the absence and in the presence of O_2. This result confirms the nature of the observed bimolecular process being an electrophilic substitution. The relative importance of the k_{10} term in eq 18 increases as the chromium concentration increases. At high ($>10^{-4}$ M) concentrations the chain pathway becomes predominant.

It is noted that the complexes with primary alkyl groups behave differently toward iodine compared to those with aralkyl and secondary alkyl groups. This difference is related to the ease of oxidation of a given class of these complexes and by the different stabilities of the corresponding free radicals. Aralykl and secondary alkyl groups are more electron donating than primary alkyl groups, resulting in more oxidizable organochromium complexes. Also, the greater stability of secondary and aralykl radicals compared to primary alkyls makes the homolysis of the organochromium(IV) macrocycle (eq 12) occur more readily. Both of these factors facilitate the chain process for the secondary alkyl- and aralkylchromium macrocycles and disfavor that for the primary alkyl complexes.

Acknowledgment. We are grateful to Dr. Lee M. Daniels of the Iowa State University X-ray Structures Laboratory for solution of the crystal structure. This research was supported by the U.S. Department of Energy, Chemical Sciences Division, under Contract W-7405-Eng-82.

Supplementary Material Available: Tables of positional parameters and their standard deviations (SI), and k_{obs} at various concentrations (SII) (4 pages); table of values of F_o and F_c in *hkl* order (7 pages). Ordering information is given on any current masthead page.

(20) $ABTS^{2-}$ = 2,2′-azinobis(3-ethylbenzothiazoline-6-sulfonate) ion.